2
10/6/78

Technical Publications and Art
Division, 8265, for TIC (2)

SAND78-8726
Unlimited Release

MASTER

Rayleigh Temperature Profiles in a Hydrogen Diffusion Flame

J. R. Smith

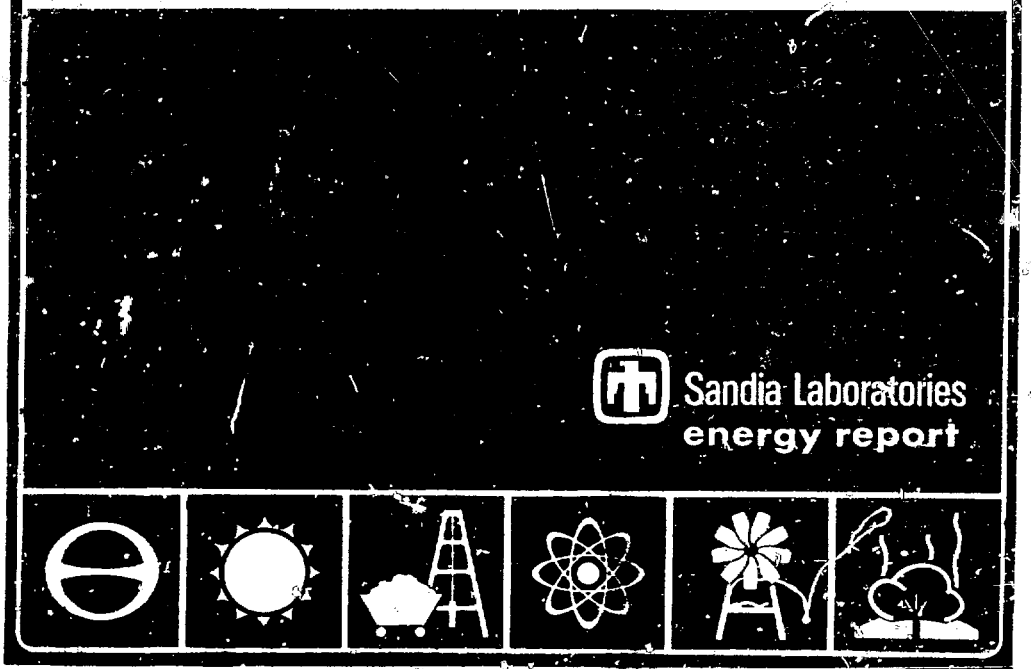

RAYLEIGH TEMPERATURE PROFILES IN A HYDROGEN DIFFUSION FLAME*

J. R. Smith
Sandia Laboratories
Livermore, California 94550

Abstract

Rayleigh scattering from a hydrogen-air laminar jet diffusion flame in combination with a numerical model of the flame has been used to determine temperature profiles. The model predictions of species concentration are used to calculate a mean Rayleigh cross-section which is used to relate the Rayleigh scattered intensity to temperature. Using an argon ion laser producing 7.5 watts at 488 nm and an optical multichannel analyzer (OMA), the scattered light was imaged into a spectrometer. The OMA was rotated 90 degrees to its normal orientation, allowing scans to be taken along the spectrometer exit slit. This resulted in a spatially resolved Rayleigh signal along the laser beam through the entire flame. Spatial resolution of 0.18 mm on each of the 500 detector elements with good signal-to-noise ratios was achieved even with integration times of only 0.03 second. Since the entire profile is made simultaneously, particulate perturbed profiles are easily recognized and discarded. Transverse profiles are presented to show flame structure. Axial profiles are compared to radiation corrected thermocouple measurements.

Introduction

Detailed modeling of combustion processes offers the hope of understanding the complex interactions of fluid mechanical mixing and chemical reactions that occur in flames. Such modeling efforts require experimental data to quantify their accuracy and lend credibility to model extrapolations. At Sandia Livermore, Miller and Kee[1] have recently modeled a laminar hydrogen-air diffusion flame which differed in some details from Raman scattering measurements of the flame as reported by Aeschliman and Cummings.[2] The Raman data indicated that the flame was significantly wider and hotter than the model predictions. These differences motivated an independent experimental study using Rayleigh scattering to determine temperature profiles. Although Rayleigh scattering has been used[3-5] in flames before, elastic scattering from particulates and differences in Rayleigh cross sections of both reactants and combustion products limit its utility. This experiment was performed in a clean room to reduce particulates to a minimum. The multiplex detector technique used also allows recognition of particulate signals and as will be discussed later, even restricts their influence on the total signal. The contributions to the Rayleigh signal by the various species in the flame are taken into account by using the model predictions of species concentration. It will be shown that there are relatively large regions in a laminar flame where uncertainties in species concentration have little effect on Rayleigh temperature measurements.

Theory

The differential cross section for Rayleigh scattering at 90 degrees from the incident light is given by[6]

$$\frac{d\sigma}{d\Omega} = \frac{2\pi^2(\mu-1)^2}{N_o^2\lambda^4} \tag{1}$$

where μ is the index of refraction of the gas at STP, $N_o = 2.69 \times 10^{19}$ cm^{-3} is a Loschmidt number, and λ is the wavelength in cm.** The effective Rayleigh differential cross section of a gas mixture is the sum of the mole fraction weighted cross sections:

$$\left(\frac{d\sigma}{d\Omega}\right)_{eff} = \sum_i X_i \left(\frac{d\sigma_i}{d\Omega}\right) \tag{2}$$

Here the mole fraction, X_i term is taken from the numerical model, and is a function of both axial and radial position in the flame. In practice, only major species H_2, N_2, O_2, and H_2O need be included in the summation since radical concentrations are always small in the hydrogen air flame.

*This work was supported by the US Department of Energy under Contract AT(29-1)789.

**Note that the use of equation (1) tacitly assumes that depolarization ratios are small, which is the case for the major species involved.

The Rayleigh scattered intensity is therefore

$$I_s = CI\, N\Omega\ell \left(\frac{d\sigma}{d\Omega}\right)_{eff} \tag{3}$$

where C is a calibration constant of the collection optics, I the incident laser intensity, N the molecular number density, Ω the solid angle of the collection optics, and ℓ the length of laser beam imaged onto the detector. Since the effective differential cross section and number density are a function of location in the flame, the scattered intensity, I_s is also a function of position. The ideal gas equation-of-state describes the relationship between the pressure, P the number density and the absolute temperature, T

$$P = \frac{N}{A_o} RT \tag{4}$$

where A_o is Avogadro's number and R is the universal gas constant. The static pressure is constant in a low velocity jet; thus the number density is inversely proportional to the temperature.

Solving equation (4) for the number density, substituting it into equation (3) and rearranging yields an explicit expression for temperature

$$T = \frac{CI\Omega\ell}{I_s} P\left(\frac{A_o}{R}\right)\left(\frac{d\sigma}{d\Omega}\right)_{eff} \tag{5}$$

If the scattered intensity, I_o is measured at a known temperature, T_o (for example, room temperature far from the flame) and the differential cross sections normalized by the effective cross section at the known point, equation (5) may be simplified further to

$$T(r,x) = \frac{T_o\left(\frac{d\sigma}{d\Omega}(r,x)\right)_{eff}}{\left(\frac{I_s(r,x)}{I_o}\right)\left(\frac{d\sigma}{d\Omega}\right)_o} \tag{6}$$

where the spatial dependence of the scattered intensity and temperature have been included. The procedure for determining temperature in the flame is thus reduced to computing the effective differential Rayleigh cross section based on the species concentrations predicted by the numerical model and measuring the Rayleigh scattered light intensity for each point of interest relative to that of the unheated air well outside the flame.

Experimental Arrangement and Procedure

The burner to produce the flame was a straight, vertical tube of 6.35 mm inside diameter with the outer surface tapered to a narrow lip at the top. The hydrogen was regulated to a constant flow rate of 19 cm^3/sec which yields a parabolic velocity profile at the tube outlet with a centerline velocity of approximately 600 cm/sec. The burner was mounted on a precision traverse to allow accurate vertical adjustment of the axial distance, between the burner tip and the horizontal laser beam. The entire experiment was located in a down flow, clean room to minimize the number of particulates in the air entrained by the flame. (As long as the plumbing was not disturbed, the hydrogen flow showed no indication of particulates.) The fans in the clean room were stopped for a few minutes before and during the time that measurements were taken. This allowed the flame to stabilize and yet entrain virtually particulate-free air.

The optical arrangement used is shown in Figure 1. A 7.5 watt, 488 nanometer laser beam was focused with a 500 mm focal length lens above the burner tip to give a long cylindrical scattering region. This configuration provides a beam of less than 0.25 mm diameter over a 75 mm length. Apertures and light traps were carefully placed to minimize scattered light due to sources outside the scattering volume from entering the collection optics.

The collection optics were chosen to image the scattering volume into the entrance slit of a 3/4 meter spectrometer. A dove prism was used to rotate the horizontal image of the scattering volume to the vertical entrance slit. These optics demagnified the image of the volume by a factor of about seven. An Optical Multichannel Analyzer® (OMA), Princeton Applied Research Model 1205D, was mounted at the exit plane of the spectrometer to scan vertically. Thus a 0.18 mm length of the scattering volume was imaged onto each of the 512 channels of the OMA for a total field of view of 92 mm. It was necessary, however, to restrict the spectrometer entrance slit height to 10 mm to improve stray light rejection which resulted in a total field of view of about 74 mm. The edges of two knife blades,

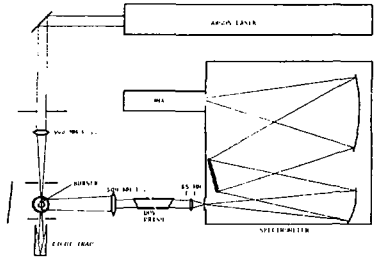

Fig. 1. Plan view of optical arrangement.

separated by a 40 mm spacer, were placed above the burner partially in the attenuated laser beam to give a scattered light signal from their location. In this manner the average width of the image on each channel (0.18 mm) was determined.

The spectrometer entrance slit width was 0.2 mm, giving a spectral resolution of 0.2 nanometers. This resolution assures complete collection of the elastically scattered light while rejecting the rotational Raman lines of the major species. The spectrometer also rejected most of the faint blue continuum of the hydrogen flame due to the reaction $H + OH \rightarrow H_2O + h\nu$.[7]

The spatial variation of the sensitivity of the optical system was about 20 percent in a smooth cosine-like distribution. The sensitivity variation was easily accounted for by normalizing by the Rayleigh signal from room air with the flame off. The Rayleigh signal was recorded as an analog signal on a CRT display and on a digital printer. Although the analog displays are presented in the next section as typical data, actual computation of temperatures used the digital output. Good signal-to-noise ratios were achieved with the 1/30 second single frame integration time of the OMA. However, 3 second integration times were used to reduce the Poisson counting statistics uncertainty of the lowest signals to the one percent level. Since the saturation level of the 1205D OMA is 750 counts and the Rayleigh signal from room air was about 500 counts per channel (on a single frame), the signal from a particle passing through the scattering volume was "clipped" at the saturation count. This means that a particle can only contribute a few hundred counts to the approximately 40,000 counts of the total integrated signal. Such a contribution is equivalent to less than 12 K even in the hottest part of the flame. It is unlikely that the signal from more than one particle was ever present on a single channel due to the clean room conditions. Also a particle traveling at a vertical velocity of 100 cm/sec would have a residence time of only 250 microseconds in the scattering volume. Therefore, it would never be seen for more than one frame.

As was previously mentioned, there are large regions in a hydrogen-air diffusion flame where uncertainty in the species concentrations does not significantly affect the use of Rayleigh scattering to determine temperature. This statement can be appreciated by examination of Figure 2 which contains both the numerical model predictions of concentrations and the resultant effective Rayleigh cross section at an axial distance of 10 mm above the burner. Note that the effective cross section is still 90 percent of the air value at the reaction zone near the 6.5 mm radius. Therefore, the region from the reaction zone outward requires little correction due to species concentration. One would expect a similar situation in all laminar diffusion flames. Along the centerline of the hydrogen-air flame relatively large corrections are necessary due to the small Rayleigh cross section of the hydrogen. Since vibrational Raman temperature measurements are difficult in air below 800 K due to small first vibrational level populations, Rayleigh scattering greatly complements such data.

Results

Figure 3 shows the change in Rayleigh signal at several axial positions. These are analog profiles that have not been normalized by the optical system sensitivity. (Hence, the roll-off of the signal at large radii.) From equation (6) we expect a low signal to imply high temperature except in the center where the hydrogen reduces the signal.

The temperature profiles calculated from the digital data at $x = 10$ mm and $x = 20$ mm axial distance are presented in Figures 4 and 5, respectively. Also included are the

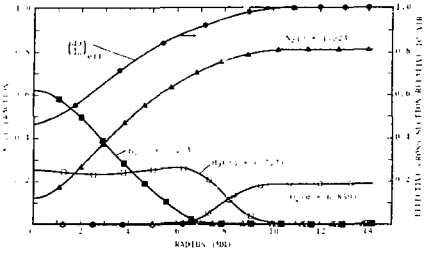

Fig. 2. Numerical model predictions of species concentrations and effective Rayleigh cross section at x = 10 mm above burner.

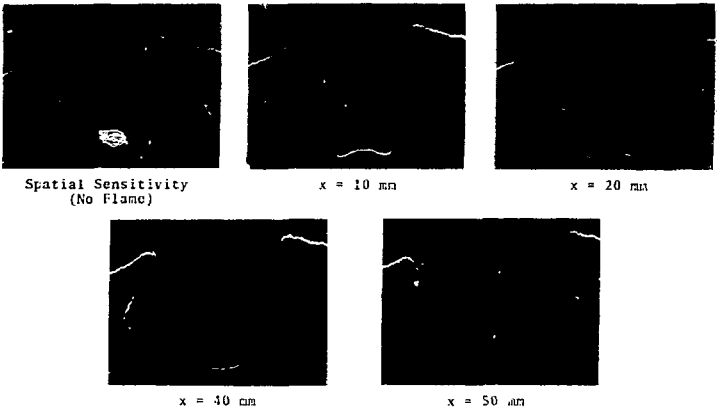

Fig. 3. Rayleigh signal radial profiles at several axial positions above burner using an integration time of 3 seconds.

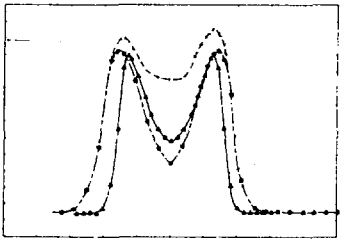

Fig. 4. Experimental and numerical model temperature profiles at x = 10 mm above burner.

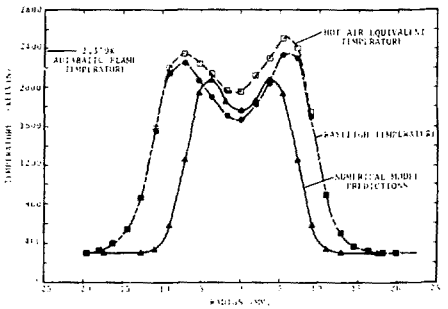

Fig. 5. Experimental and numerical model temperature profiles at x = 20 mm above burner.

model predictions of temperature profiles at these same axial positions. The Rayleigh data indeed indicate a slightly higher temperature reaction zone and a wider flame. The dashed profile in the figures is the temperature that would be calculated if $(dz/dz)_{eff} = 1$. The difference between this hot air equivalent temperature and the experimental profile is due to the correction for the species concentrations.

It was noticed from the single frame exposures that there was considerable flame "flicker" at less than the 30 Hz framing rate. To visualize this flicker, thirty consecutive profiles were overlayed on the CRT display as shown in Figure 6. The width of the profile in the vertical direction corresponds to the degree of flicker. Notice that this increases with height. Such an instability in laminar flames has been noted before by Grant and Jones.[8] The flicker is apparently a fluid instability that is independent of both Reynolds number and fuel used in a laminar flame. As such, it contributes to the appearance that the flame is wider than a stable flame. It would certainly be misleading for long integration, such as the 120 second integration necessary for the Raman data cited earlier.

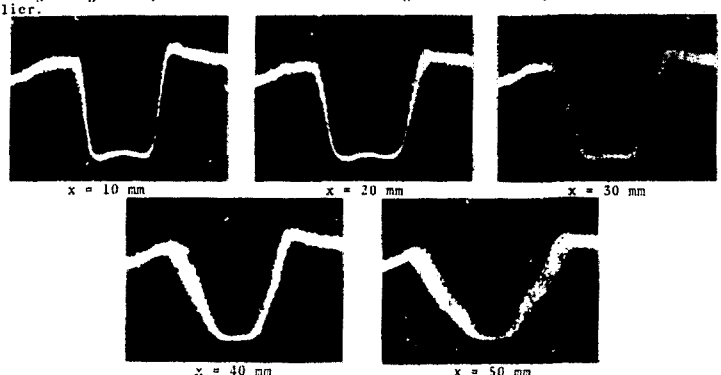

Fig. 6. Thirty sequential profiles with 1/30 second integration time showing flame "flicker".

The x = 20 mm axial position profile in Figure 6 was taken about ten minutes after the clean room fans had been off. It clearly shows how particulates are present. None of the temperature data were taken at such late times after fan shutdown.

Even accounting for flame flicker by estimating its width from short time exposures, the flame appears wider than the model predicts. This is shown in Figure 7 where the model and experimental 1500 K isotherms are compared with "flicker" estimates included on the experimental data.

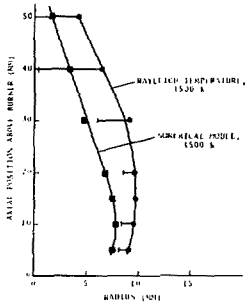

Fig. 7. Experimental and numerical model flame shape along outer 1500 K isotherm. Bars on experimental isotherm indicate magnitude of flame "flicker".

An axial temperature profile was constructed from the centerline data of the radial profiles. This data is compared with the model predictions in Figure 8. The influence on the temperature value by a ± 10 percent variation in the hydrogen concentration is denoted by the vertical bars at the x = 10 mm position where the axial hydrogen gradient was very large. The numbers at each point are the effective relative differential cross section values used. Note that the experimental evidence indicates a slightly longer and hotter flame than the model predicts.

Also included in Figure 8 are square symbols to represent axial temperatures obtained from radiation corrected thermocouple data. The thermocouple consisted of a 0.25 mm diameter bead of platinum, platinum-13 percent rhodium coated with silica to reduce catalytic effects. Due to the extremely steep temperature gradients, it is probably not practical to make radial profile thermocouple measurements. Since the thermocouple radiation correction consists of a heat transfer balance between the convective and radiative transport to the thermocouple bead, the species concentrations from the model had to be used in the convective terms. The maximum radiation correction was + 165 K at x = 35 mm. Because conduction along the thermocouple leads was not included in the correction and a high radial temperature gradient is present at the x = 5 mm position, the thermocouple indicates a temperature above the actual gas temperature.

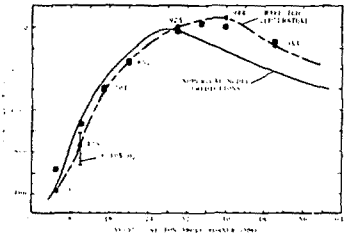

Fig. 8. Experimental and numerical model axial temperatures. Value of effective Rayleigh cross sections are indicated at each experimental point. Radiation corrected thermocouple measurements shown by ■.

Conclusions

Rayleigh scattering has been used to determine temperatures in a laminar hydrogen-air flame. The relatively large Rayleigh scattering cross sections allowed short integration times which led to the discovery of flame oscillations. These oscillations partially account for the difference between the flame model and previously reported Raman temperature measurements. However, the Rayleigh temperature data indicate a slightly longer, wider, and hotter flame than the numerical model predicts.

References

1. Miller, J. A. and Kee, R. J., "Chemical Nonequilibrium Effects in Hydrogen-Air Laminar Jet Diffusion Flames," Journal of Physical Chemistry 81, p. 2534, 1977.
2. Aeschliman, D. and Cummings, J. Jr., "Application of Raman Scattering to the Study of a Hydrogen Laminar Diffusion Flame in Air," presented at the Optical Society Annual Meeting, Toronto, Canada, October 1977.
3. Robben, F., "Comparison of Density and Temperature Measurements Using Raman Scattering and Rayleigh Scattering," Combustion Measurements in Jet Propulsion Systems, (ed., R. Goulard), Project SQUID Workshop Proceedings PU-RI-76, Purdue University, p. 179, May 1975.
4. Pitz, R. W., Cattolica, R. J., Robben, F., and Talbot, L., "Temperature and Density in a Hydrogen-Air Flame from Rayleigh Scattering," Combustion and Flame 27, p. 313-320, 1976.
5. Cattolica, R. J., Robben, F., and Talbot, L., "The Interpretation of the Spectral Structure of Rayleigh Scattered Light from Combustion Gases," AIAA 14th Aerospace Sciences Meeting, AIAA paper No. 76-31, January 1976.
6. Shardanand and Prasad Rao, A. D., "Absolute Rayleigh Scattering Cross Sections of Gases and Freons of Stratospheric Interest in the Visible and Ultraviolet Regions," NASA TND-8442 Wallops Flight Center, March 1977.
7. Padley, P. J., "The Origin of the Blue Continuum in the Hydrogen Flame," Transactions of the Faraday Society, Vol. 56, p. 451-454, 1950.
8. Grant, A. J. and Jones, J. M., "Low-Frequency Diffusion Flame Oscillations," Combustion and Flame 25, p. 153-160, 1975.